KERNFORSCHUNGSZENTRUM

KARLSRUHE

August 1971 KFK 1480

On the Potential of Advanced Gamma-Ray Spectrometers for Nuclear Material Assay

W. Michaelis, C. Weitkamp

KERNFORSCHUNGSZENTRUM KARLSRUHE
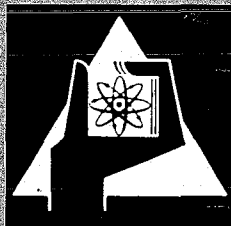
August 1971   KFK 1480

Geschäftsführung
Technisch-Wissenschaftliche Koordination und Planung

Institut für Angewandte Kernphysik

On the Potential of Advanced Gamma-Ray Spectrometers
for Nuclear Material Assay

W. Michaelis and C. Weitkamp

Gesellschaft für Kernforschung mbH

Abstract

Cost-effectiveness optimization for the application of Compton suppression
techniques in nondestructive nuclear material assay requires quantification
of the basic spectroscopic parameters. The influence of peak-to-background
ratio and window setting and some aspects of data processing are studied
in detail. The results are applied to typical spectra at various stages of
the fuel cycle.

It turns out that in the case of unirradiated fuel there is no need for the
use of anti-Compton devices for the determination of U^{235} in plutonium-free
fuel, of U^{238} and of Pu^{239}. The technique is, however, most useful in the
assay of U^{235} in mixed U-Pu fuel and in the determination of plutonium
isotopes other than Pu^{239}.

Considerable advantages are also offered in gamma spectrometry on spent
fuel and in the analysis of delayed spectra from active neutron interrogation.

The capabilities of Compton rejection spectrometry may be used either to
shorten the counting time or improve statistical accuracy, or to reduce count-
rate losses.

Detectors from high-Z material may compete with germanium detectors even
if the high-Z detectors do not match volume and resolution specifications
of germanium. Futher development in this field deserves all possible support.

Zusammenfassung

Die Kosten-Nutzen-Optimierung für die Anwendung der Compton-Reduktionstechnik
auf die zerstörungsfreie Bestimmung von Kernbrennstoffen erfordert eine Quanti-
fizierung der grundlegenden spektroskopischen Parameter. Der Einfluß des
Signal-Untergrund-Verhältnisses und der Fensterlage sowie einige in Zusam-
menhang mit der Meßdatenverarbeitung auftretenden Fragen werden ausführlich
untersucht und die Ergebnisse auf typische Spektren, wie sie auf verschie-
denen Stufen des nuklearen Brennstoffzyklus anfallen, angewandt.

Dabei zeigt sich, daß im Falle unbestrahlten Brennstoffs keine Notwendigkeit
für den Einsatz einer Anti-Compton-Anordnung besteht, solange U^{235} in pluto-
niumfreien Brennstoff, U^{238} oder Pu^{239} bestimmt werden sollen. Die Technik
ist dagegen überaus nützlich für die U^{235}-Bestimmung in U-Pu-Mischbrennstoff
und bei der Messung anderer Plutoniumisotope als Pu^{239}.

Das Verfahren ist auch bei der Gammaspektrometrie abgebrannten Brennstoffs
und bei der Analyse verzögerter Spektren nach der Bestrahlung mit Neutronen
von großem Nutzen.

Die Möglichkeiten der Compton-Reduktions-Technik können zur Verkürzung der
Meßzeit, zur Verbesserung der statistischen Genauigkeit oder zur Verminderung
von Zählratenverlusten genutzt werden.

Detektoren aus Stoffen hoher Ordnungszahlen können schon bei kleinen Volumina
und schlechter Auflösung in der erreichbaren Genauigkeit mit Germanium-Detek-
toren konkurrieren. Weitere Entwicklungsarbeiten auf diesem Gebiet sollten
jede mögliche Unterstützung genießen.

1. Introduction

Since the effectiveness of a rational and objective safeguards system depends strongly upon the availability of procedures for detection, identification and analysis of nuclear material, intensive research and development of both destructive and nondestructive measurement techniques for nuclear safeguards applications were started and have been in progress for the past five years. In these studies particular emphasis has been placed on gamma-ray spectroscopy as a nondestructive method which provides distinct signatures of the relevant nuclear species. For routine applications nondestructive methods must fulfill several essential requirements: The counting times must be short, the measurements should offer a sufficiently precise and accurate information and there should be a reasonable cost-effectiveness relationship.

In the earlier measurements sodium iodide scintillation detectors have been extensively used for the assay of nuclear fuel material. With improving resolution and sensitivity capabilities of semiconductor counters these devices have more and more replaced the scintillation detectors. Significant impulses have come in this process from the rapid development of nuclear spectroscopy in decay and reaction studies. Here, the necessity to analyse very complex gamma-ray spectra has finally led to the construction of advanced semiconductor instruments, such as the Compton suppression or anti-Compton spectrometer. In addition, considerable effort has been devoted to the development of detectors from high-Z semiconductor materials.

It is the purpose of this working paper to discuss some aspects of the capabilities of advanced gamma-ray spectrometers with respect to safeguards applications and to arrive at some quantification of the progress which may be achieved. Problems of spectrum analysis and data

processing are closely connected to this discussion. Since gamma-ray spectrometry can be used at almost all stages of the fuel cycle, very different spectrum shapes and structures, energy regions and counting rates have to be considered. Particular emphasis will be given to passive assay methods, because these techniques offer the advantages of relatively simple instrumentation and are, in general, adaptable to portable equipment for use by a travelling inspector. The discussion of active interrogation methods will be restricted to some recent measurements which allow a quantative estimate of the future potential in safeguards applications. It is not intended to investigate the problems associated with gamma-ray self-absorption in the fuel material.

2. Compton-Suppression Detector Systems

Only part of the gamma rays which may be utilized in safeguards spectrometry measurements have sufficiently low energies for the photoeffect being the dominant interaction process in the detector material. In general, the presence of strong Compton scattering affects the subsequent processing of the spectrum data. Even at low energies the accuracy and counting time may suffer considerably, if nuclear species emitting gamma rays of higher energy are present in the source.

The Compton suppression technique provides a powerful means to improve the performance of the spectrometer system. The arrangement consists of a germanium detector which is surrounded by a large plastic or sodium iodide scintillator. In the commonly used configuration, the gamma rays are collimated into the central semiconductor detector. If a Compton event occurs in this counter, the scattered photon will be detected in the surrounding secondary counter with reasonable probability. By operating the two detectors in coincidence, Compton events can be identified and rejected from the pulse-height analysis.

Such anti-Compton spectrometers have been constructed in a variety of geometries and designs with, accordingly, different reduction factors in the peak-to-background ratio.[1-5][+] Improvements of this ratio by a factor of up to 10 have been achieved and systems with even higher reduction factors are under construction.[6]

A typical gamma-ray spectrum as obtained with an anti-Compton spectrometer is shown in Fig. 1. The pulse-height distribution is characterized by a very low background under the peaks which only slightly increases with decreasing energy in spite of the fact that several hundreds of gamma rays with energies above the sectional display shown contribute to the Compton background. This performance was obtained by ensuring a strong absorption of gamma rays scattered in the forward direction. The anti-Compton shield consisted of a 50 cm diam. x 40 cm plastic scintillator (NE 102 A) with the germanium counter (5 cm^3) in its centre, and a 4 in. diam. x 6 in. sodium iodide detector placed within a well directly behind the vacuum chamber of the semiconductor diode. Of course, such a system can hardly be used as a portable instrument. It is therefore necessary to analyse carefully the requirements in safeguards applications and to find a compromise between efficient background reduction and simplicity in design. The optimization is facilitated by the fact that in the passive assay of unirradiated fuel the gamma-ray energy is limited to 1 MeV. In measurements on spent fuel the intensity decreases very rapidly with increasing energy. Thus a sodium iodide shield with moderate dimensions and optimized geometrical layout will be preferred.

In nuclear research the main objectives of anti-Compton spectrometry are the precise determination of gamma-ray energies and intensities and the detection of weak gamma-ray lines which in singles mode are

----

+) Bibliography is not exhaustive. Further references will be found in
   in the literature cited.

PORTION OF A CAPTURE SPECTRUM FROM ERBIUM ENRICHED TO 95.6%
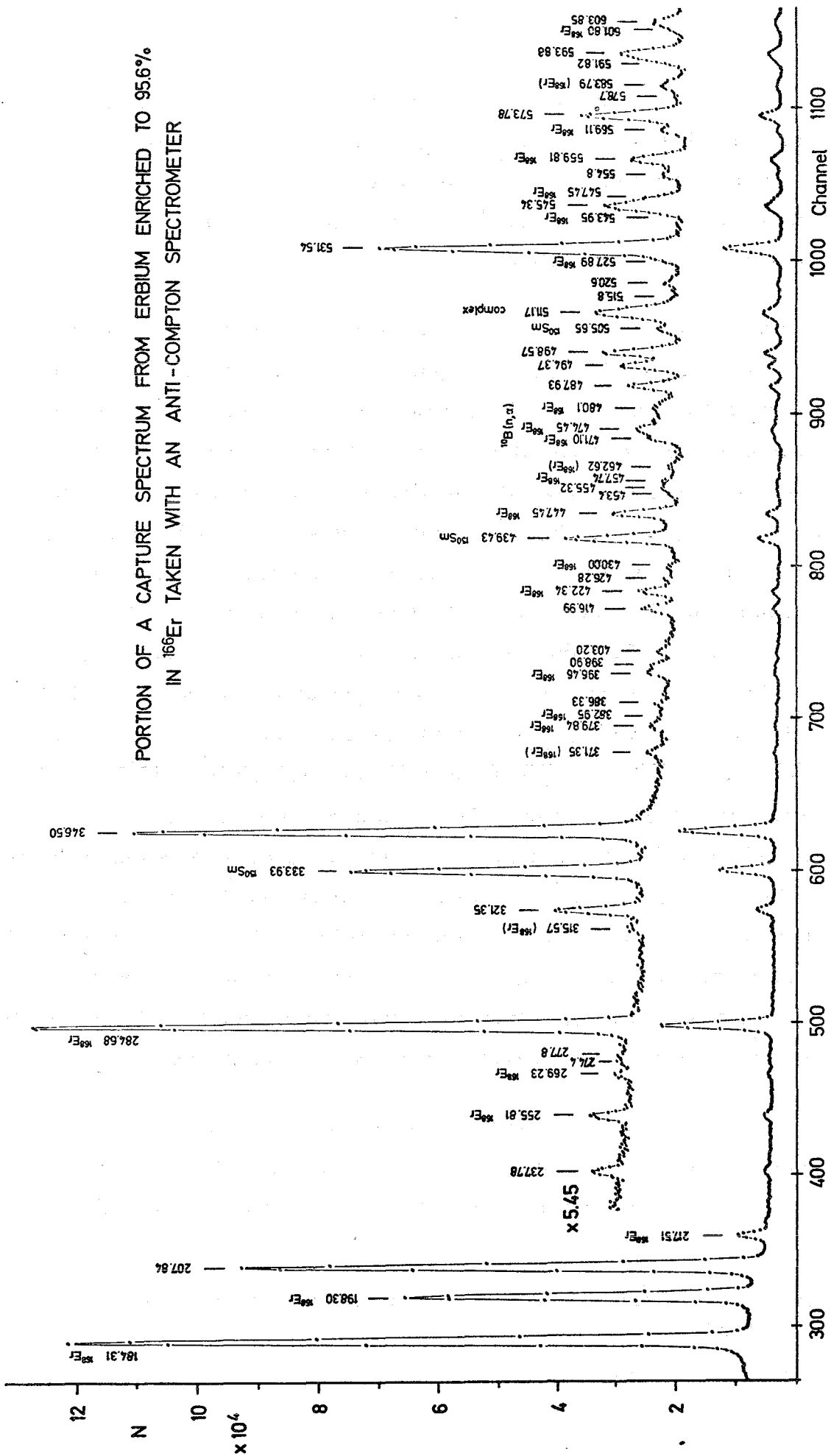IN ^{166}Er TAKEN WITH AN ANTI-COMPTON SPECTROMETER

Fig. 1: Sectional display of the gamma-ray spectrum from the reaction $Er^{166}(n, \gamma)$ taken with the Karlsruhe anti-Compton spectrometer.

obscured by the Compton background. On the other hand, in safeguards measurements use is made of well-known lines which in many cases have pronounced intensities in the pulse-height distribution, and the peak areas, or parts of them, have to be determined with a precision as high as possible. Thus the situation is quite different from that in nuclear research. The usefulness of anti-Compton spectrometry will depend on the stage in the fuel cycle and the type of fuel under study. Therefore, it is believed to be conducive to analyse in some detail the influence of the peak-to-background ratio on the most important measuring parameters.

3. Peak-to-Background Ratio and Spectrometer Performance

Let us assume that the analysis of the gamma-ray spectrum is performed by setting a "peak window" on the relevant gamma line and two "background windows" on the neighbouring Compton background.[+] As will be shown below, this kind of analysis may be preferable to the usual fitting procedure.

In order to improve the statistics for the background determination, the secondary windows should be chosen as broad as possible. Using the definitions explained in Fig. 2 the useful number of counts in the peak window, P, may be obtained from

$$P = T - B, \tag{1}$$

where T is the total number of counts in the peak window and B is the corresponding background determined from $B^* = \beta B$, the number of background counts in the secondary windows ($\beta > 1$, if possible). With the peak-to-background ratio

$$\alpha = \frac{P}{B} \tag{2}$$

+) In very complex spectra it may be necessary to use only one background window.
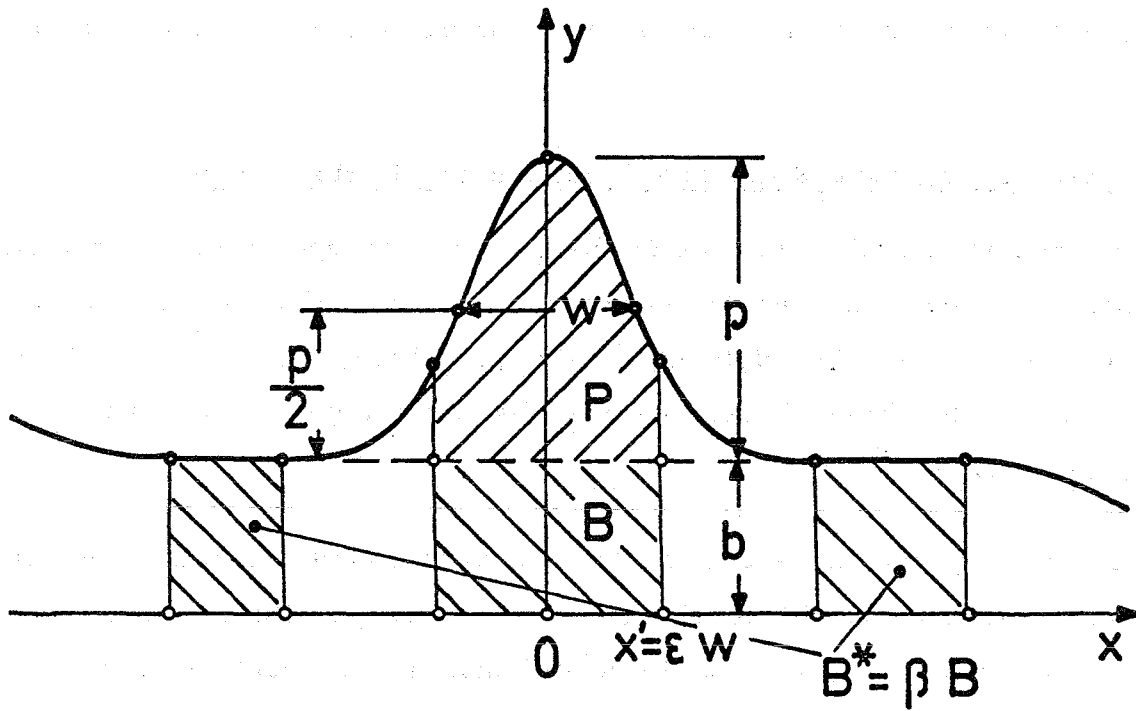
Fig. 2: Portion of gamma spectrum showing Gaussian photopeak superimposed on smooth background for definition of parameters.

and the error equation

$$\delta P = \sqrt{\delta T^2 + \delta B^2} = \sqrt{T + B/\beta} \tag{3}$$

we can calculate the relative error in P by means of the formula

$$\frac{\delta P}{P} = \frac{1}{\sqrt{P}} \sqrt{1 + \frac{1}{\alpha} + \frac{1}{\alpha\beta}} . \tag{4}$$

For $\beta = 1$ eq. (4) reduces to

$$\frac{\delta P}{P} = \frac{1}{\sqrt{P}} \sqrt{1 + \frac{2}{\alpha}} . \tag{5}$$

These formulae describe the enhancement of the relative error in the peak area determination due to the background under the peak.

Let P' be the peak area for $0 < \alpha < \infty$ and P the peak area in the case of zero background ($\alpha = \infty$); then we get for equal relative errors

$$\frac{P'}{P} = 1 + \frac{1}{\alpha} + \frac{1}{\alpha\beta} . \tag{6}$$

Eq. (6) yields the factor by which the useful number of counts in the peak window must be increased in the presence of background in order to achieve the same precision as may be reached under background-free conditions. This requires a corresponding enhancement of either the counting time or the counting rate. Accordingly, a reduction of the background by Compton suppression may be used either to shorten the measuring time, to reduce the counting rate or to improve the precision of the measurement.

In correspondence to eq. (6) we obtain for the total numbers of counts, assuming again equal relative errors in the peak area determination,

$$\frac{T'}{T} = (1 + \frac{1}{\alpha} + \frac{1}{\alpha\beta}) \ (1 + \frac{1}{\alpha}) . \tag{7}$$

This formula describes the increase in the total number of counts within the peak window due to finite peak-to-background ratios.

Values for P'/P and T'/T as a function of the peak-to-background ratio and the background window setting ß have been listed in Table 1. In order to facilitate interpolation, the functions (P'/P-1)x100 and (T'/T-1)x100 have been plotted in Fig. 3 and 4, respectively.

Table 1

Influence of peak-to-background ratio and window
setting on useful and total number of counts in the
peak window

ß	0.5	1	2	5	0.5	1	2	5
α		P'/P				T'/T		
∞	1.00	1.00	1.00	1.00	1.00	1.00	1.00	1.00
50	1.06	1.04	1.03	1.02	1.08	1.06	1.05	1.04
20	1.15	1.10	1.08	1.06	1.21	1.16	1.13	1.11
10	1.3	1.20	1.15	1.12	1.43	1.32	1.27	1.23
5	1.6	1.40	1.30	1.24	1.92	1.68	1.56	1.49
3	2.0	1.67	1.50	1.4	2.67	2.22	2.00	1.87
2	2.5	2.00	1.75	1.6	3.75	3.00	2.63	2.4
1.5	3.0	2.33	2.0	1.8	5	3.89	3.33	3.0
1.0	4	3	2.5	2.2	8	6	5	4.4
0.5	7	5	4.0	3.4	21	15	12	10.2
0.2	16	11	8.5	7	96	66	51	42
0.1	31	21	16	13	341	231	176	143

As can be seen from these data, unfavourable background conditions may lead to considerably lengthened counting times, to very high counting rates with possibly associated count-rate losses or, alternatively, to insufficient precision of the measurement.

$$\left(\frac{P'}{P} - 1\right) \times 100$$

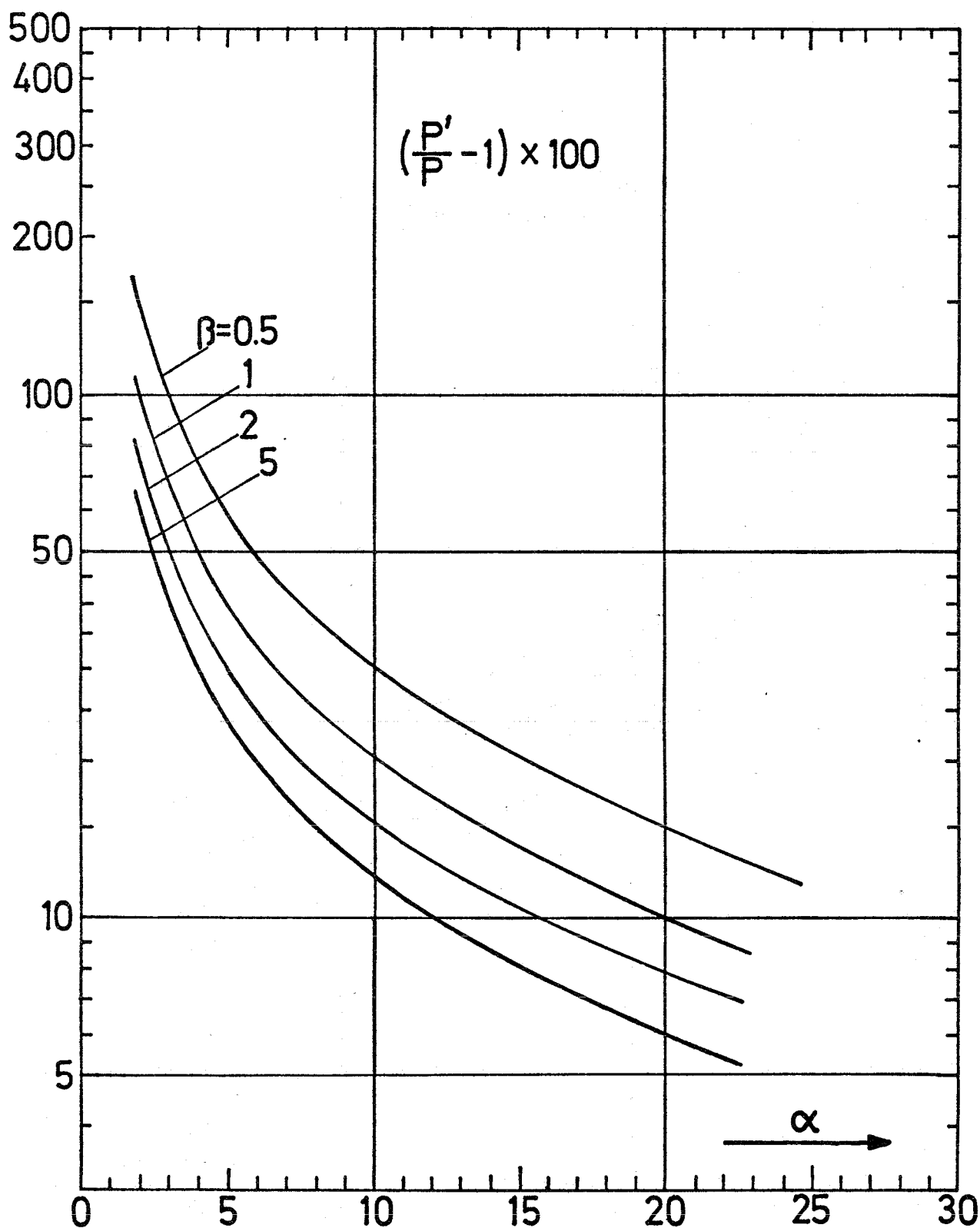Fig. 3: Excess peak area (in percent) necessary for obtaining the same precision as in the background-free case, as a function of the peak-to-background area ratio α, for different relative side window widths β.

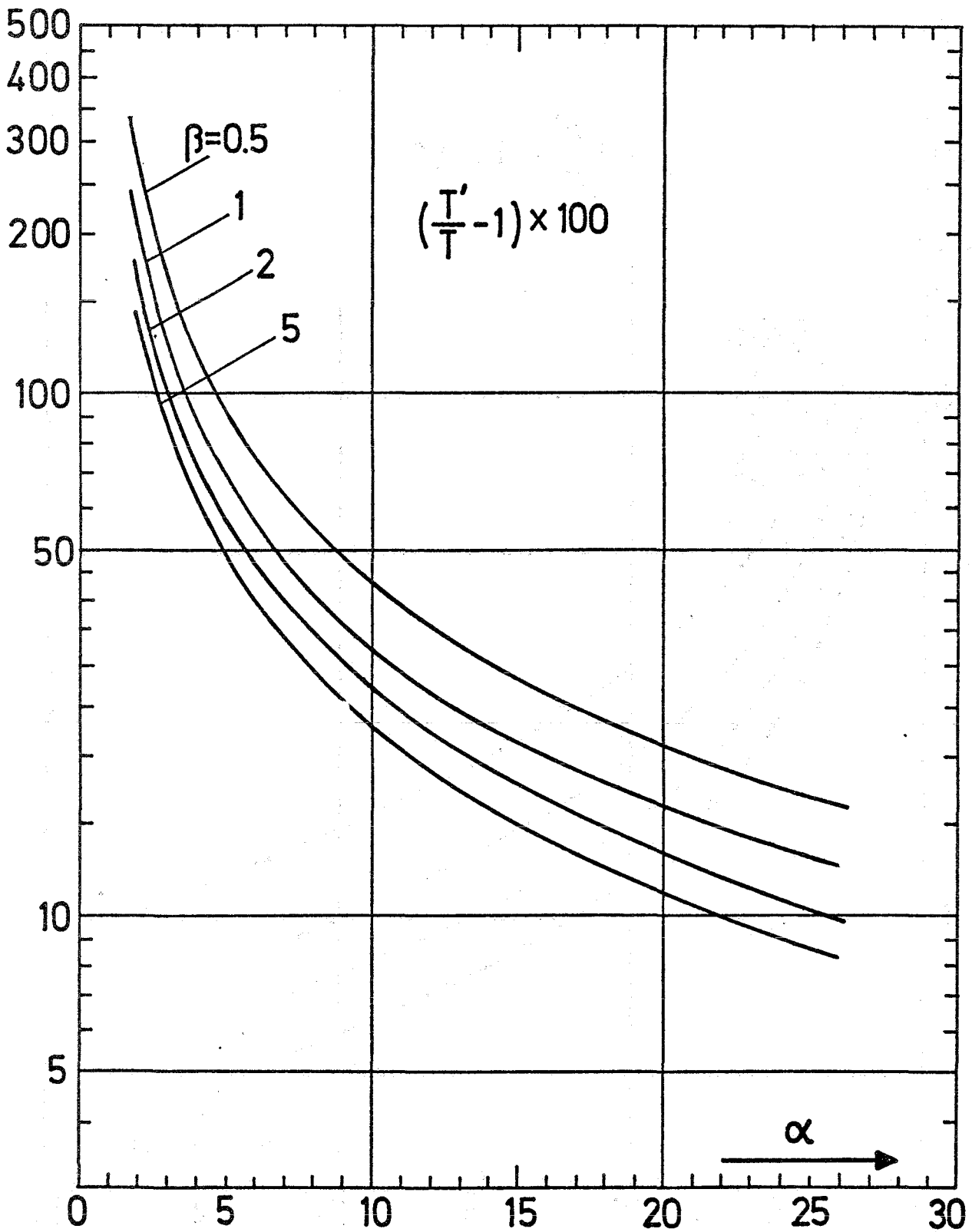$$\left(\frac{T'}{T}-1\right)\times 100$$

Fig. 4: Excess total area in peak window (in percent) for equal precision as in the background-free case, as a function of α for different values of ß.

Let us assume that the line shape (number of counts y vs signal amplitude x) can be represented by a Gaussian function

$$y(x) = p\ e^{-x^2 (\frac{w^2}{4\ln 2})^{-1}}.$$ (8)

Here, p is the peak amplitude and w the half-width. Then, the peak area P can be obtained by integration of eq. (8). For symmetric window setting and with $\varepsilon = x'/w$ (cf. Fig. 2) we get

$$P = \frac{p\ w}{2}\ \sqrt{\frac{\pi}{\ln 2}}\ \text{erf}\ (2\ \sqrt{\ln 2}\ \varepsilon).$$ (9)

B, the number of background counts within the peak window, may be calculated from

$$B = 2\ b\ w\ \varepsilon,$$ (10)

with b = amplitude of the background.

Combination of eqs. (9) and (10) yields

$$\alpha = \frac{1}{4}\ \sqrt{\frac{\pi}{\ln 2}}\ \frac{\text{erf}\ (2\ \sqrt{\ln 2}\ \varepsilon)}{\varepsilon}\ \ \alpha' = f\ (\varepsilon)\alpha',$$ (11)

where α' is the amplitude ratio p/b which can be easily deduced from the experimental pulse-height distributions displayed in the literature. The function $f(\varepsilon)$ has been plotted in Fig. 5 vs the percentage of the total peak area covered by the window setting.

Eq. (11) and Fig. 5 together with formula (4) indicate that it may be advantageous to utilize only a fraction of the peak area for spectrum analysis. It can be shown that there is a flat minimum in the relative error $\mathcal{d}P/P$ as a function of the fractional peak area selected by the window. For small values of α' the minimum is found between 60 and
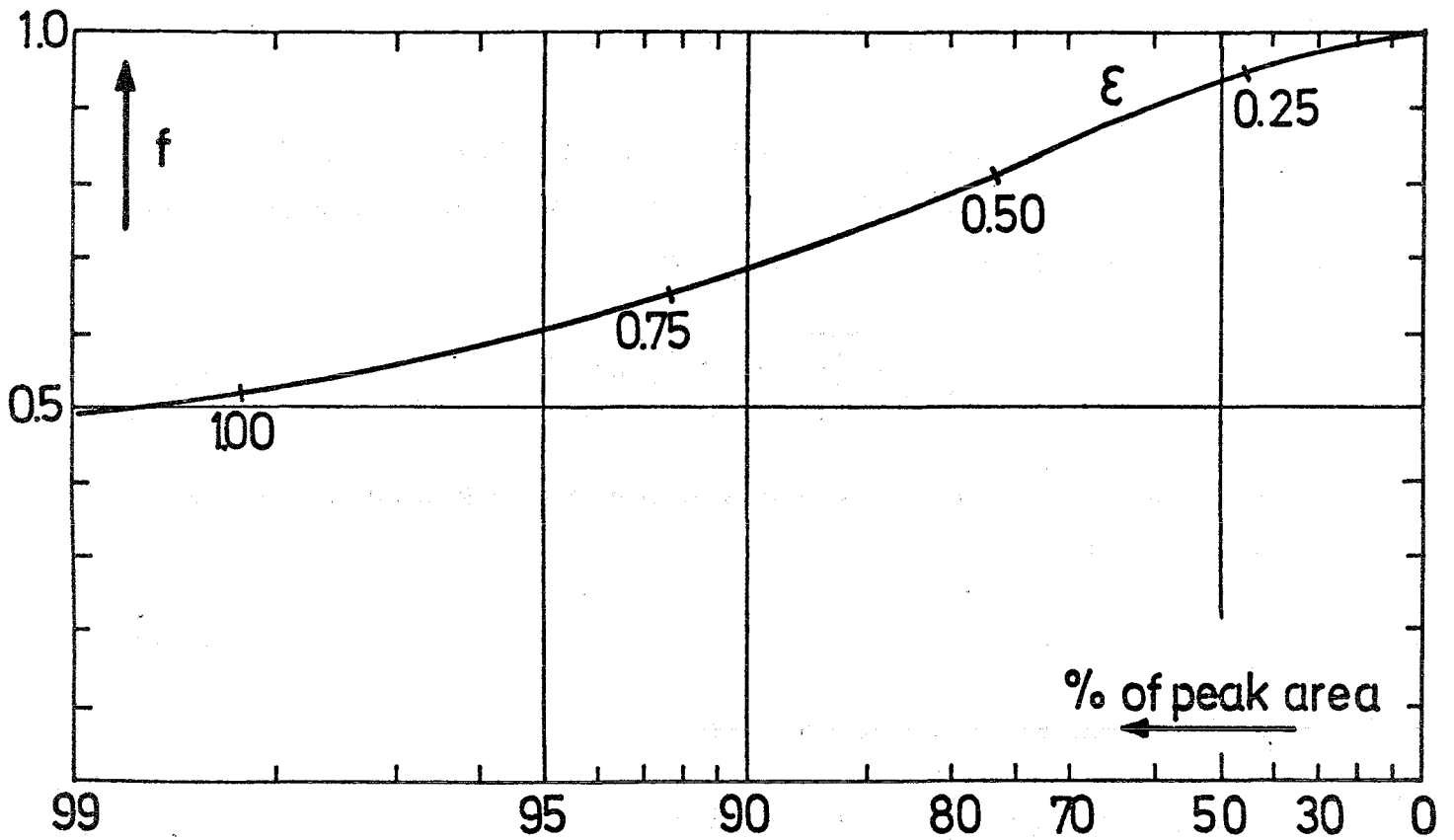
Fig. 5: Parametric plot of the function f and the percentage of the area of the whole peak as a function of the relative peak window width $\varepsilon = x' / w$.

80 % of the peak area. With increasing α' this effect becomes insignificant. The optimization of dP/P may be easily combined with the advantages inherent in on -line spectrum analysis by means of digital windows and direct counting.

4. Passive Assay of Uranium Isotopes

The formalism described in the preceding section has been applied to typical measuring problems in fuel assay in order to work out quantitatively the usefulness of Compton suppression techniques at the various stages of the fuel cycle. Although there are many publications on gamma-ray measurements, the information which can be evaluated for these purposes is still limited, since many reports suffer from the lack of detail in experimental parameters such as amount of source material, source-to-detector distance, counting time, detector volume, presence and absence of count-rate losses, etc. Also for practical purposes it was preferred to select realistic sources such as rods, plates or platelets instead of highly purified samples.

A survey on the evaluated data is given in Table 2. The following symbols have been used:

d = source-to-detector distance,

$t_{1\%}$ = counting time to obtain 1 % statistical accuracy in singles mode,

c.r.l. = count-rate losses, presence or absence denoted by + or -,

P/P_∞ = fraction of total peak area covered by the peak window,

G_P = gain in peak area P for constant dP/P, if the peak-to-background ratio α is improved by a factor of 5,

G_T = gain in the total number of counts within the peak window, if the peak-to-background ratio α is improved by a factor 5,

ACS = anti-Compton spectrometer.

A

TABLE 2

Survey on gamma spectrometry data from various fuel materials

Detected Isotope	E_γ [keV]	Source Type	Source Dim. [mm]	Source Comp. [%]	Ref.	d [cm]	$t_{1/2}$ [min] theor./exp.	Detector Ge(Li)	c.r.l.	α'	α	P/P_∞ [%]	β	P'/P	T'/T	G_P [%]	G_T [%]	Conclusion ACS
1	2	3	4	5	6	7	8	9	10	11	12	13	14	15	16	17	18	19
U^5	186	rod^a	11.7 ⌀	$2U^5+U^8$	7	10.3	5.4/5.2	20 cc	−	8.4^c	6.7	78	1	1.29	1.49	18	26	(+)
		rod^{ab}	11.7 ⌀	$2U^5+0.5Pu+U^8$	7	10.3	6.2/6.9	20 cc	+	4.8^c	3.8	78	1	1.53	1.93	27	39	+
		rod^{ab}	11.7 ⌀	$2U^5+1Pu+U^8$	7	10.3	7.5/7.7	20 cc	+	3.3^c	2.6	78	1	1.80	2.48	36	50	+
		rod^a	11.7 ⌀	$2.5U^5+U^8$	7	10.3	4.1/3.9	20 cc	−	10.9^c	8.7	78	1	1.23	1.37	15	22	(+)
		rod^{ab}	11.7 ⌀	$2.5U^5+0.5Pu+U^8$	7	10.3	4.7/5.0	20 cc	+	6.3^c	5.0	78	1	1.40	1.68	23	33	+
		rod^a	11.7 ⌀	$3U^5+U^8$	7	10.3	3.3/3.1	20 cc	−	13.0^c	10.4	78	1	1.19	1.31	13	19	(+)
		rod^{eb}	5.73 ⌀	$3U^5+10Pu+U^8$	7	10.3	83.5/−	20 cc	+	0.6^c	0.54	60	1	4.71	13.4	63	82	+
		rod^{eb}	5.73 ⌀	$18U^5+10Pu+U^8$	7	10.3	4.6/−	20 cc	+	3.2^c	2.9	60	1	1.70	2.30	33	47	+
U^8	1001	platelet^f	50.68^{2}x1.57	U_{nat}	7	2.2	18.8/19.5^g	20 cc	−	≈40^c	≈28	89	5	1.04	1.08	3	5	−
		platelet^f	50.68^{2}x1.57	$20U^5+80U^8$	7	2.2	21.6/23.8^g	20 cc	−	≈40^c	≈28	89	5	1.04	1.08	3	5	−
Pu^9	414	rod^{eb}	5.73 ⌀	$3U^5+10Pu+U^8$	7	2.5	6.3^i/5.6^g	20 cc	−	28.6^h	22.9	78	2	1.07	1.11	6	8	−
		rod^{eb}	5.73 ⌀	$25Pu+U^8$	7	2.5	2.5^i/2.2^g	20 cc	−	32.1^h	25.7	78	2	1.06	1.10	5	7	−
Pu^1	208^j	rod^{ab}	11.7 ⌀	$2.5U^5+0.5Pu+U^8$	7	10.3	6.8/−	20 cc	+	7.9^h	6.3	78	1	1.31	1.53	19	27	+
		rod^{eb}	5.73 ⌀	$3U^5+10Pu+U^8$	7	10.3	1.7/−	20 cc	+	8.1^h	6.5	78	1	1.30	1.51	18	26	+
		rod^{ak}	11.7 ⌀	$2.5U^5+0.5Pu+U^8$	−^{1}	10.3	215/−	20 cc	+	0.8	0.64	78	1	4.13	10.6	61	80	+
Pu^1/Pu^9	148	thin	10 mm^2	Pu^1/Pu^9	8	3		20 cc	?	4.7	3.8	78	1	1.53	1.93	27	39	+
	129	layer		= 0.0126						5.2	4.2	78	1.	1.47	1.82	25	37	+
Cs^4/Cs^7	796	2M19^m		highly	9	≥6 ft		35 mm	?	1.1	1.0	60	1	3.0	6.0	53	72	+
	662			enr. U^5				x1.6 cm^2		1.9	1.7	60	1	2.18	3.47	44	60	+
Rh^6	622	sample^n		U^5	4	?		?	?	≈0.18	≈0.16	60	2	10.4	75	72	91	+
		sample^o		U^5	4	?		?	?	≈0.72	≈0.65	60	2	3.3	8.4	55	77	+
		sample^p		Pu^9	4	?		?	?	≈3.7	≈3.3	60	2	1.46	1.88	25	38	+
f.p.^{q}	832	rod^{rt}	8.6 mm ⌀	90.4 Pu^9	7	10	47x2/−	20 cc	?	0.42	0.38	60	1	6.27	22.7	67	86	+
		rodst	8.6 mm ⌀	92.9 U^5	7	10	16x2/−	20 cc	?	0.71	0.64	60	1	4.13	10.6	61	80	+
	975	rod^{rt}	8.6 mm ⌀	90.4 Pu^9	7	10	64x2/−	20 cc	?	0.57	0.51	60	1	4.93	14.6	64	83	+
		rodst	8.6 mm ⌀	92.9 U^5	7	10	49x2/−	20 cc	?	0.55	0.50	60	1	5.0	15.0	64	83	+
	1032	rod^{ru}	8.6 mm ⌀	90.4 Pu^9	7	10	208x5/−	20 cc	?	0.34	0.31	60	1	7.46	24.0	69	88	+
		rod^{su}	8.6 mm ⌀	92.9 U^5	7	10	31x5/−	20 cc	?	0.67	0.60	60	1	4.34	11.6	62	81	+
	1642	rod^{ru}	8.6 mm ⌀	90.4 Pu^9	7	10	86x5/−	20 cc	?	0.81	0.73	60	1	3.74	8.9	59	78	+
		rod^{su}	8.6 mm ⌀	92.9 U^5	7	10	605x5/−	20 cc	?	0.34	0.31	60	1	7.46	24.0	69	88	+

a Oxide with ρ = 6.3 g cm^{-3}. Cladding zircaloy. LWR fuel.

b Pu isotopic abundances = 90.875 % Pu^9, 8.223 % Pu^0, 0.856 % Pu^1, 0.040 % Pu^2

c FWHM = 2.1 keV at 122 keV; 2.8 keV at 1275 keV.

d Theoretical values calculated on the basis of the window setting in column 12-14 assuming the absence of count rate losses.

e Oxide with ρ = 6.3 g cm^{-3}. Cladding 0.5 mm stainless steel. Fast reactor fuel.

f SNEAK platelets.

g Deduced from experimental data given in the literature.

h FWHM = 2.1 keV at 122 keV; 2.2 keV at 511 keV.

i Can be further reduced by about a factor of 2 by including the 375 keV group in the analysis.

j U^{237}.

k Abundance of Pu^1 as given in footnote^b reduced by a factor of 10.

l All values extrapolated from rod^{ab}.

m Spent MITR fuel element after 9 month cooling.

n Irradiated to 5% burn up at a flux of 2x10^{13} n cm^{-2} sec^{-1}. Cooling time 180 days.

o Irradiated to 50% burn up at 2x10^{13} n cm^{-2} sec^{-1}. Cooling time 250 days.

p Irradiated to 70% burn up at 2x10^{13} n cm^{-2} sec^{-1}. Cooling time 180 days.

q Fission product gamma rays from active interrogation

r Plutonium oxide.

s Uranium oxide

t 2 min irradiation at a thermal flux of 10^7 n cm^{-2} sec^{-1}; cooling time 2 min; measuring time 2 min.

u 2 min irradiation at a thermal flux of 10^7 n cm^{-2} sec^{-1}; cooling time 5 min; measuring time 5 min.

The other symbols have been explained in section 3. The abbreviations U^5, U^8, Pu^9, Pu^1, Cs^4, Cs^7 and Rh^6 stand for U^{235}, U^{238}, Pu^{239}, Pu^{241}, Cs^{134}, Cs^{137} and Rh^{106}, respectively.

The theoretical values for $t_{1\%}$ have been calculated on the basis of the window settings specified in column 12 - 14 assuming the absence of count-rate losses. The agreement with experimental results is surprisingly good. The ratio α' has been deduced from the spectra shown in the cited literature. For calculating G_P and G_T we have intentionally assumed a Compton suppression system of only moderate performance. The gain in peak area may be utilized to shorten the counting time or to improve the accuracy of the measurement. G_T is a measure of the possible reduction in the total counting rate and thus, in particular, may serve to eliminate count-rate losses. This is very important for obtaining precise and reliable spectrometric data.

The measurements in ref.[7] on the detection of U^{235} by means of the 186 keV gamma ray have been performed with a source-to-detector distance of 10.3 cm. Application of an anti-Compton spectrometer will not require an increase of this distance. Thus the data in Table 2 are directly relevant. As can be seen from column 17 and 18, the ACS is only of limited value in the case of plutonium-free LWR fuel. However, with increasing plutonium content $t_{1\%}$ increases due to the enlargement of the background, and remarkable count-rate losses have been observed in spite of processing only a small section of the pulse-height distribution. Here, the Compton suppression technique can be used with great success. U^{235} in fast reactor fuel is hardly accessible to gamma spectrometric determination in reasonable counting times without applying background suppression. The measuring time may be reduced by a factor up to 3 and the total counting rate by a factor up to 5.

As to the assay of U^{238}, Table 2 clearly demonstrates that anti-Compton

spectrometry will be of no advantage. The peak-to-background ratio for the 1001 keV gamma ray is sufficiently high in singles mode and, for energy reasons, other heavy isotopes do not affect the measurement. ß may be chosen quite high, since the background exhibits no structure at this energy.

5. Passive Assay of Plutonium Isotopes

Best suited for passive assay of Pu^{239} is the 414 keV gamma ray which is emitted with an intensity of 3.4×10^4 photons per sec and g Pu^{239}. The peak-to-background ratio is quite favourable (Table 2) and, in contrast to the low-energy region (cf. section 4), no count-rate losses occur even for commonly used fast reactor fuel. Reasonable counting times can be achieved. Other isotopes have only little influence on the measurement. Thus Compton suppression does not offer any significant advantage.

Pu^{241} may be detected by means of the 208 keV gamma ray arising from the decay of the U^{237} (6.75 d) daughter nucleus. In this energy region Pu^{239} considerably contributes to the background under the peak. For both LWR and fast reactor fuel rods count-rate losses have been observed in ref.[7] with a 20 cc detector in spite of processing only a small section of the pulse-height distribution. The source-to-detector distance was 10.3 cm in these measurements. This distance can also be realized in anti-Compton spectrometry. The main advantages will be the reduction of count-rate losses and the achievement of reasonable counting times in the case of small Pu^{241} abundances (Table 2).

Determinations of the isotopic ratio Pu^{241}/Pu^{239} are usually performed by comparing gamma-ray intensities from these nuclides with the energies being chosen close together so as to minimize differences in absorption. Well suited are the gamma rays at 148 keV and 129 keV from Pu^{241} and Pu^{239}, respectively. The experimental situation is similar to that

in the assay of U^{235} and Pu^{241} by means of the 186 keV and 208 keV gamma rays. In practical applications attention has to be paid to the count rate and Compton suppression may successfully be used to reduce both count-rate losses and measuring time.

6. Gamma Spectrometry on Spent Fuel

Analysis of the gross fission product gamma-ray spectrum offers the possibility to determine the fission ratio from uranium and plutonium, to compare the post-irradiation data with pre-irradiation assay, to measure the residual fuel content and to obtain information on the irradiation history of the fuel. Of particular interest are the product nuclides Cs^{134}, Cs^{137} and Ru^{106}. While Cs^{137} is produced by simple decay of the 137 mass chain, Cs^{134} arises from a two-step process: the end product Cs^{133} of the 133 mass chain has a significant capture cross section which leads to the production of Cs^{134}. Ru^{106} is characterized by a striking difference in the fission yield from U^{235} and Pu^{239}.

Column 11 of Table 2 shows that the peak-to-background ratios, even for the intense gamma rays from these nuclides, are very low.[+] Since the source strength is high enough to use a well-collimated gamma beam the use of the Compton suppression technique will allow a considerable improvement of the spectroscopic data in the assay of spent fuel. Even a system of only moderate performance will shorten the counting time by factors up to 4, and the total number of counts may be reduced by an order of magnitude. In contrast to the assay of unirradiated fuel high-energy gamma rays, in general, contribute appreciably to the background under the peak. This has to be taken into account in the geometric layout of the Compton rejection system.

[+] Ru^{106} decays with 1 y half-life to Rh^{106} without gamma-ray emission. It is detected via the decay of the short-lived daughter nucleus which has a half-life of 30 sec. - α' for Rh^{106} in singles mode has been deduced from spectra taken using a Compton rejection annulus with a background reduction by about a factor of 3.6 (ref.[4]).

7. Active Interrogation

Delayed gamma-ray spectra from active neutron interrogation of plutonium and uranium rods have recently been studied at Karlsruhe[7] in great detail. The measurements have been performed under experimental conditions that are close to those in safeguards applications. They provide sufficient information to allow the examination of the future potential of this technique. Active interrogation offers the advantage that the gamma-rays emitted, due to their higher energy, undergo much less self-absorption than those in passive assay.

In order to be suitable for safeguards measurements, the gamma-ray lines should attain a high statistical accuracy in short counting times and the intensity should be sufficiently different for U^{235} and Pu^{239}. The spectroscopic data for the most promising gamma rays have been analysed in Table 2. The gamma rays at 832 keV and 975 keV show the best intensities, but only moderate discrimination power. The lines at 1032 keV and 1642 keV are weaker the intensities being, however, quite different for U^{235} and Pu^{239}. In all cases the values for G_P and G_T indicate that Compton suppression spectrometers will considerably improve the measurements. The counting time may be reduced to one third of the value in singlesmode without loss of accuracy, and the total number of counts that has to be processed can be lowered by approximately one order of magnitude. The spectroscopic situation is similar to that in spent fuel assay.

Since, for physical reasons, the counting time is limited to 2 min and 5 min, respectively, $t_{1\%}$ has been factorized in column 8, in order to make clear the necessary increase in count rate for 1 % accuracy of single peak areas in routine applications. For practical cases it must be taken into account that LWR fuel contains only about 3 % of fissile material but that, on the other hand, due to self-absorption in highly

enriched fuel, the expected count rates are only down a factor of 4 or so. This means that for the worst of the cases of Table 2 (U^{235} determination from the 1642 keV gamma ray) the ratio of thermal flux to the flux used in ref.[7] (10^7 n cm^{-2} sec^{-1}) must be increased by a factor of about 2 400. The gain from an anti-Compton spectrometer being $\geq 1/0.31$ (from column 17 in Table 2), this factor can be reduced to ≤ 750 bringing the total thermal flux to 7.5×10^9 n cm^{-2} sec^{-1}. This flux cannot be produced by an isotopic source of reasonable dimensions, but is easily obtained from one of the recently developed, safe and low-cost small power thermal reactors.

In the determination of the quantities of fissile material an additional source of error must be taken into account. It is due to the fact that the peak areas of the two lines, P_1 and P_2, are linear combinations of the contents in uranium and plutonium, a_5 and a_9:

$$P_i = A_i \, a_5 + B_i \, a_9 \qquad (i = 1, 2).\qquad (12)$$

The coefficients A_i and B_i must, of course, be determined experimentally from spectra taken with pure samples of uranium and plutonium. The quantities a_5 and a_9 can then be computed from eqs. (12); under the assumption that the error of A_i and B_i are negligible compared to the errors of the peak areas and that these latter ones are statistically independent, the relative error of, say, the quantity of uranium[+) is

$$\frac{\delta a_5}{a_5} = \frac{\sqrt{(k_1 + \lambda)^2 \sigma_1^2 + (k_2 + \lambda)^2 \sigma_2^2}}{|k_1 - k_2|}, \qquad (13)$$

where the following abbreviations have been used:

[+) Eq. (13) also holds for the relative plutonium error $\delta a_9 / a_9$ if either A_i and B_i in eqs. (14) and a_5 and a_9 in eq. (15) are interchanged, or in eq. (13) k_1, k_2 and λ are replaced by their reciprocals. In order not to change the meaning of the k_i and λ the second possibility was chosen for the computation of Fig. 6.

$$k_i = A_i/B_i = \quad \text{discrimination ratio of gamma ray i,} \tag{14}$$

$$\lambda = a_9/a_5 = \quad \text{plutonium-to-uranium mixing ratio,} \tag{15}$$

$$\sigma_i = \delta P_i/P_i = \quad \text{relative error of area of gamma peak i.} \tag{16}$$

Unless one of the k_i is zero, the relative error $\delta a_5/a_5$ of the quantity of uranium (or of plutonium, $\delta a_9/a_9$) clearly exceeds the smaller of the relative peak area errors σ_i and increases rapidly as k_1 and k_2 get close to each other, even for $\lambda = 0$ or ∞. It is also interesting to note that for finite λ the values of $\delta a_5/a_5$ and $\delta a_9/a_9$ are not only related to the ratio k_1/k_2 of the discrimination ratios, but decrease with increasing values of the k_i if k_1/k_2 is held constant.

For illustration relative errors $\delta a_5/a_5$ and $\delta a_9/a_9$ have been computed for a determination of U^{235} and Pu^{239} by spectroscopy of gamma rays from fission products produced with different abundance. Only pairs of gamma rays have been used for simplicity, and the two following cases were considered:

i)   the 832 keV-975 keV gamma-ray pair, with discrimination ratios of 1.92 and 1.31, and

ii) the 1032 keV-1642 keV gamma-ray pair, with discrimination ratios of 3.84 and 0.29.

Instead of showing the precision achieved for a given product of counting time and intensity, the necessary increase of this product as compared to the values used in ref. [7] for a 1 % precire determination is plotted in Fig. 6 as a function of the Pu/U mixing ratio. The same total amount of fissile material as in ref. [7] has been assumed. The figure shows that an ACS with a reduction ratio of 5 (solid lines) allows a counting time (or intensity) roughly 3 times smaller than without Compton suppression (dashed lines). It is also evident that the discrimination factors play an
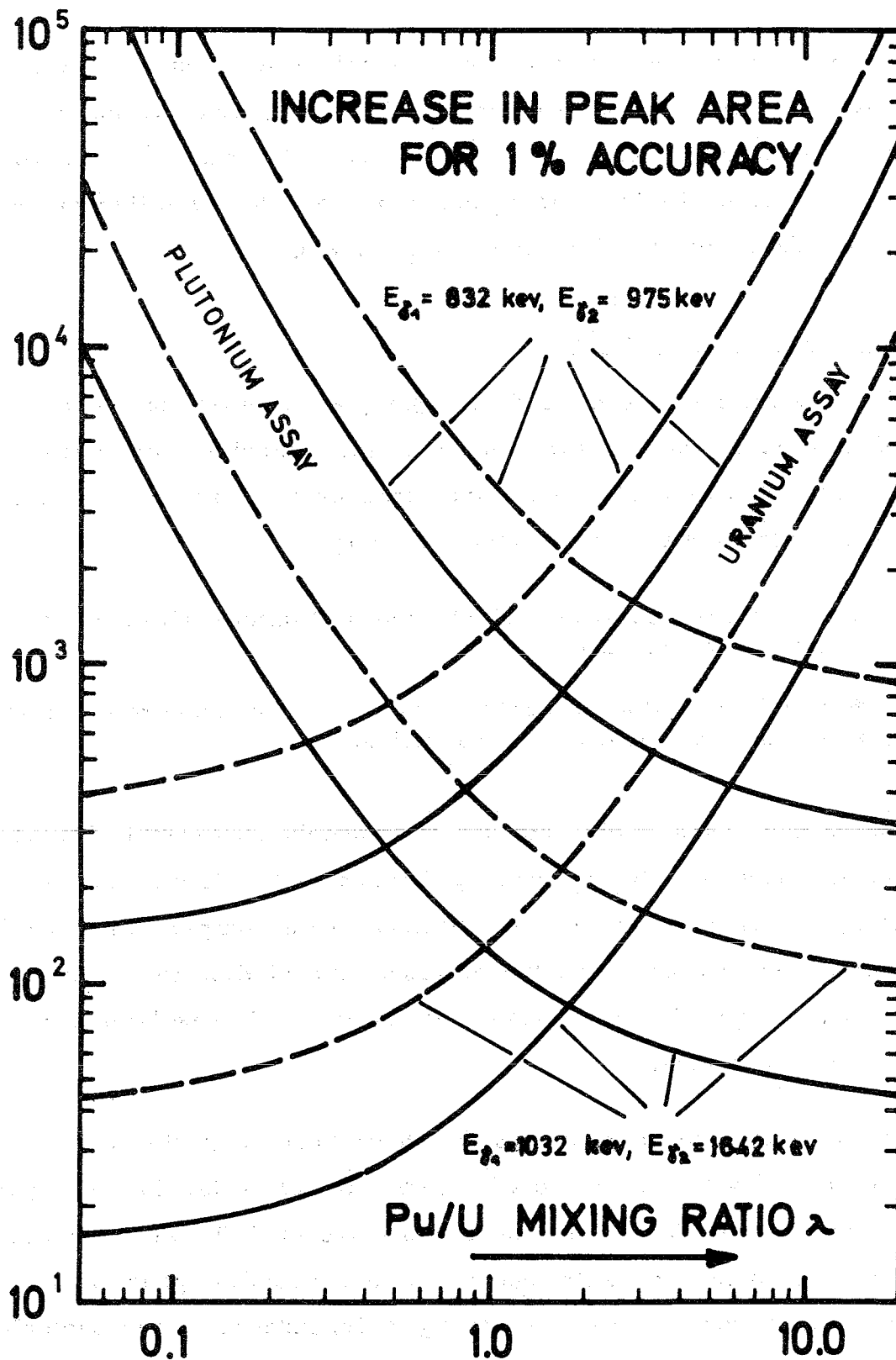
Fig. 6: Increase, relative to the values of ref. [7], of the product
counting time x intensity necessary for a determination of
U or Pu to 1 % precision as a function of the Pu/U
mixing ratio λ . Dashed curves without anti-Compton rejection,
solid curves with an ACS suppression factor of 5.

enormous role in the accuracy of the material assay. Thus the higher-energy pair of gamma rays, although much less intense, is better suited for the assay by almost a factor of ten. The same factorization has been used as in Table 2; thus this ratio, due to the different cycle times, reduces to about 5 for practical purposes.

8. High-Z Detector Materials

Soon after the advent of semiconductor gamma-ray spectrometers with Ge(Li) diodes a search for other detector materials with even better characteristics began. The main reasons for this search were two inherent drawbacks of germanium, namely

i) the necessity for operation and storage of lithium-drifted material at low temperatures, and

ii) the relatively low atomic number leading to only moderate detection efficiency and peak-to-background ratios.

This search has, as a whole, not yet been overly successful. Neither has it so far been possible to develop devices that, without the need for cooling, provide resolution and efficiency data comparable to or better than those of Ge(Li), nor have the developments of detectors from material with larger Z led to sufficiently large, well-resolving and easy-to-handle products.

Of the large catalogue of materials that have been tried the most promising with $Z > 32$ is, at present, cadmium telluride. Table 3 gives a short list of some data important for the use of CdTe as a material for gamma-ray detectors. Although resolutions are still poor, and detector volumes very small, the strong Z dependence of the photoelectric effect $(\sim Z^4)$ as compared to the Compton effect $(\sim Z)$ results not only in an increased efficiency, but also in an increased peak-to-background ratio. The effect upon the accuracy $\delta P/P$ as computed in the third paragraph of this paper (eq. 5) is thus twofold. Whether a given device

compares favourably or poorly with a Ge(Li) detector will, of course, greatly depend upon the particular application.

For getting a semiquantitative idea of what is needed in terms of volume and resolution of a CdTe detector, let us consider as an example the analysis of a mixture of about equal quantities of U^{235} and Pu^{239} by passive gamma-ray spectrometry.

Table 3

Some properties of CdTe as a material for gamma-ray spectrometers

Atomic number	48/52	(Ge for comparison: 32)
Density	6.20g cm^{-3}	(" " " $\quad$: 5.35 g cm^{-3})
Energy per electron-hole pair	4.51 eV	(" " " $\quad$: 2.95 eV)
Fano factor	?	(" " " $\quad$: 0.058)
Examples for sizes and resolutions	7.5 keV at 122 keV - 30μ layer [10] 27 % at 662 keV - 1 mm layer [11] 16 % at 662 keV - 13 mm^3 [12] no photopeaks resolved - $\approx 1 \text{ cm}^3$ [12] $\leq$ 35 keV at 500 keV - 10 mm^3 [13] 28 keV at 662 keV - 2 mm wafer x 15 mm ϕ [14]	

In order to do so we have to make a number of simplifying assumptions:

i)   Only U^{235} and Pu^{239} are present in the mixture.

ii) U^{235} emits only one gamma-ray at 186 keV, and the intensity of all Pu^{239} gamma-rays above 330 keV can be considered concentrated in one gamma line at 400 keV.

iii)   Relative discriminator window widths can be made equal:

$$\varepsilon_{CdTe} = \varepsilon_{Ge}, \quad \beta_{CdTe} = \beta_{Ge} = 1 .$$

iv)   Only small detectors are used; this means that attenuation and multiple events can be neglected, and peak and background count-rate ratios are determined by the ratios of the corresponding cross sections.

v)   The Compton distribution may be approximated by a rectangle extending from zero to the Compton edge energy.

Although some of these assumptions are hard to justify from a physical point of view, the result may be used as an order-of-magnitude estimate of when CdTe will start to compete with conventional gamma detection devices.

The quantity to compare is the relative accuracy of the 186 keV photo-peak determination which, from eq. (5), is given by

$$\frac{\delta P}{P} = \frac{1}{\sqrt{P}} \sqrt{1 + \frac{2}{\alpha}} \; , \; \text{with } \alpha = \frac{P}{B} \; .$$

Now P and B of the 186 keV gamma-ray are given by

$$P_{mat} = c \; \varphi(\varepsilon) \; I^{186} \; \sigma^{186}_{ph \; mat} \; \rho_{mat} \frac{1}{A_{mat}} \; V_{mat} \quad \text{and} \quad (17)$$

$$B_{mat} = c \; \frac{\varepsilon w^{186}_{mat}}{E^{400}_c} \; I^{400} \; \sigma^{400}_{c \; mat} \; \rho_{mat} \; \frac{1}{A_{mat}} \; V_{mat} \; , \quad (18)$$

where superscripts refer to the gamma-ray energies and subscripts to the Compton and photoeffect or to the material, CdTe and Ge.
$\varphi(\varepsilon) = P/P_{\infty}$ is the fraction of the photopeak measured with relative window setting ε , w is the peak FWHM, I is the gamma-ray intensity, σ the cross section, ρ the density, A the molecular weight, V the detector volume, and c is a constant taking care of solid angle effects etc. Again, self-absorption in the source is not considered.

With the appropriate values for the A, ρ and σ's inserted in eqs. (17)

and (18) the ratio of relative accuracies computed from eq. (5) is given by

$$\left(\frac{\delta P}{P}\right)_{CdTe} \Big/ \left(\frac{\delta P}{P}\right)_{Ge} = 0.2 \frac{(\varphi(\varepsilon)V)_{Ge}\left[1 + 0.0032\ j\ (\frac{\varepsilon w}{\varphi(\varepsilon)\ keV})_{CdTe}\right]}{(\varphi(\varepsilon)V)_{CdTe}\left[1 + 0.0144\ j\ (\frac{\varepsilon w}{\varphi(\varepsilon)\ keV})_{Ge}\right]} . \quad (19)$$

We use the intensity ratio

$$j = I^{400} / I^{186} = 3.07 \quad (20)$$

computed from the data of Cline[15] and the above assumption ii), with

$$\varepsilon_{CdTe} = \varepsilon_{Ge} = 1 \qquad \text{corresponding to}$$
$$\varphi_{CdTe} = \varphi_{Ge} = 0.982 \quad (21)$$

(see Fig. 5) and FWHM $w_{Ge}^{186} = 1.5$ keV which respresents a conservative estimate. Then the requirement of equal performance for the two kinds of detectors, obtained by setting the right-hand side of eq. (19) equal to unity, leads to the relation

$$V_{CdTe}/V_{Ge} = \frac{1}{550}\ \frac{w_{CdTe}}{keV} + \frac{1}{5.5} . \quad (22)$$

Table 4 shows for what resolution (at 186 keV) what size of CdTe detector can be tried to replace a Ge(Li) detector of given volume.

Table 4

Volume, in cm^3, of a CdTe detector of resolution (FWHM) w_{CdTe} needed to replace a Ge(Li) detector of volume V_{Ge} for the uranium measurement in a mixture of equal quantities of ^{235}U and Pu^{239} computed under a variety of simplifying conditions.

V_{Ge}	$0.1\ cm^3$	$0.3\ cm^3$	$1\ cm^3$	$3\ cm^3$
w_{CdTe} = 2 keV	0.02	0.06	0.19	0.56
5 keV	0.02	0.06	0.19	0.57
10 keV	0.02	0.06	0.20	0.60
20 keV	0.02	0.07	0.22	0.65
50 keV	0.03	0.08	0.27.	0.82

The figures show that even small detectors of high-Z material may be very useful for this particular application, and that further development in the field deserves all possible support.

9. Summary

Cost-effectiveness optimization for the application of Compton suppression techniques in nondestructive nuclear material assay requires quantification of the basic spectroscopic parameters. The influence of peak-to-background ratio and window setting and some aspects of data processing are studied in detail. The results are applied to typical spectra at various stages of the fuel cycle.

It turns out that in the case of unirradiated fuel there is no need for the use of anti-Compton devices for the determination of U^{235} in plutonium-free fuel, of U^{238} and of Pu^{239}. The technique is, however, most useful in the assay of U^{235} in mixed U-Pu fuel and in the determination of plutonium isotopes other than Pu^{239}.

Considerable advantages are also offered in gamma spectrometry on spent fuel and in the analysis of delayed spectra from active neutron interrogation.

The capabilities of Compton rejection spectrometry may be used either to shorten the counting time or improve statistical accuracy, or to reduce count-rate losses.

Detectors from high-Z material may compete with germanium detectors even if the high-Z detectors do not match volume and resolution specifications of germanium. Further development in this field deserves all possible support.

References:

1. W. Michaelis and H. Küpfer, Nucl. Instr. and Meth. <u>56</u> (1967) 181.

2. W. Michaelis and F. Horsch, Neutron Capture Gamma-Ray Spectroscopy, IAEA, Vienna, 1969, p. 35.

3. P. Suominen, University of Jyväskylä, Research Report Nr. 5/1970.

4. R. L. Heath, Proc. Symp. on Safeguards Research and Development, WASH - 1076 (1967) 115.

5. H. Fiedler and O. Teuch, Ge(Li) Gamma Spectrometer Systems, Canberra Industries, Inc. (1968).

6. W. Michaelis, U. Fanger and D. Heck, KFK-Ext. Bericht 1/70-1.

7. J. Wolff, Diplomarbeit, Karlsruhe (1970), to be published.

8. J. Peter and H. Schumacher, Journ. Nucl. Energy <u>23</u> (1969) 617.

9. N. C. Rasmussen, Proc. Symp. on Safeguards Research and Development, WASH - 1076 (1967) 130.

10. E. N. Arkard'eva, L. V. Maslova, O. A. Matveev, S. M. Ryvkin and Yu. V. Rud', IEEE Transactions on Nuclear Sience 15, No. 3 (1968) 258.

11. V. S. Vasilov, R. Kh. Vagapov, V. A. Chapnin and M. V. Chukichev, Atomnaja Energija <u>28</u> (1970) 505.

12. K. Zanio, J. Neeland and H. Montano, IEEE Transactions on Nuclear Science <u>17</u> (1970) No. 3, 287.

13. K. R. Zanio, Hughes Research Laboratories, Report SAN-549-6 (1970).

14. R. O. Bell, N. Hemmat and F. Wald, IEEE Transactions on Nuclear Science, <u>17</u> , No. 3 (1970) 241.

15. J. E. Cline, Idaho Nuclear Corporation Report IN - 1448 Rev. (1971).